Geofile 2018-3

Geochronologic data from samples collected in the Turtle Lake area, NTS 104M/16, northwest British Columbia

By: Mitchell G. Mihalynuk, Richard M. Friedman, Nancy Joyce, Alfredo Camacho, and Alex Zagorevski

Recommended citation:
Mihalynuk, M.G., Friedman, R.M., Joyce, N., Camacho, A., and Zagorevski, A., 2018. Geochronologic data from samples collected in the Turtle Lake area, NTS 104M/16, northwest British Columbia. British Columbia Ministry of Energy, Mines and Petroleum Resources, British Columbia Geological Survey GeoFile 2018-3
http://www.empr.gov.bc.ca/Mining/Geoscience/PublicationsCatalogue/GeoFiles/Pages/GF2018-3.aspx [Accessed: year, month, day].

Contents

This document outlines the contents of Geofile 2018-3, which includes raw geochronological and related data in 64 files. The contents are:

- this overview document, plus tabular geochronological and related data for each of:
  - 3 samples analyzed by Chemical Abrasion - Thermal Ionization Mass Spectroscopy (CA-TIMS)
  - 2 samples analyzed by Sensitive High Resolution Ion MicroProbe (SHRIMP)
  - 2 detrital zircon samples analyzed by Laser Ablation - Inductively Coupled Plasma - Mass Spectroscopy (LA-ICPMS)
    - including 50 cathodoluminescence images (9 grains imaged from one sample and 41 grains from the other sample)
  - 4 samples analyzed by $^{40}Ar/^{39}Ar$ step heating
    -including separate analyses of biotite and hornblende for each of two samples
    File names and formats follow:

1. *Geofile2018-3 GEMGeochron.pdf* (this document)
2. *Geofile2018-3 GEMgeochron*MMI16-6-2CATIMS.*xls*
   (Excel format workbook containing four worksheets)
3. *Geofile2018-3 GEMgeochron*MTS16-1-4cCATIMS.*xls*
   (Excel format workbook containing four worksheets)
4. *Geofile2018-3 GEMgeochron*MMI16-18-1CATIMS.*xlsx*
   (Excel format workbook containing four worksheets)
5. *Geofile2018-3 GEMgeochron*DMI16-5-1aSHRIMP.*xls*
   (Excel format workbook containing four worksheets)
6. *Geofile2018-3 GEMgeochron*MMI16-16-9SHRIMP.*xls*

(Excel format workbook containing four worksheets)

7. *Geofile2018-3 GEMgeochron*MTS16-24-13LA.*xls*
   (Excel format workbook containing eleven worksheets)
8. *Geofile2018-3 GEMgeochron*MMI16-8-1LA.*xls*
   (Excel format workbook containing eleven worksheets)
9. *Geofile2018-3 GEMgeochron*MMI16-14-9ArBt.*xls*
   (Excel format workbook containing two worksheets)
10. *Geofile2018-3 GEMgeochron*MMI16-14-9ArHb.*xls*
    (Excel format workbook containing four worksheets)
11. *Geofile2018-3 GEMgeochron*MMI16-20-16ArBt.*xls*
    (Excel format workbook containing two worksheets)
12. *Geofile2018-3 GEMgeochron*MMI16-20-16ArHb.*xls*
    (Excel format workbook containing two worksheets)
13. *Geofile2018-3 GEMgeochron*MMI16-29-05Ar.*xls*
    (Excel format workbook containing three worksheets)
14. *Geofile2018-3 GEMgeochron*MTS16-24-23Ar.*xls*
    (Excel format workbook containing four worksheets)

Geofile 2018-3 synopsis

Geofile 2018-3 contains the results, methodology and quality control data from geochronological analyses of samples collected during fieldwork conducted as part of the Federal Geo-mapping for Energy and Minerals (GEM) program near the British Columbia – Yukon border, in the Atlin area. GEM generates new public geoscience in support of exploration for energy and mineral resources, and in support of northern communities, for more informed, science-based decisions about their land, economy and society. The British Columbia Geological Survey of the Ministry of Energy, Mines and Petroleum Resources, has been an active partner in GEM projects in BC since their inception. Partnered activities focus on the transition of porphyry environments between BC and Yukon and the geological framework of ancient oceanic crust.

In 2016, systematic quadrangle mapping activities conducted under GEM focused on a critical boundary segment between Stikine volcanic arc and Cache Creek oceanic crustal terranes in the Turtle Lake area northwest of Atlin (Mihalynuk et al., 2018). Results of that mapping, and implications of most of the data included in this Geofile, are discussed in Mihalynuk et al. (2018). Geological frameworks for the samples dated are provided in Mihalynuk et al. (2017, 2018) and some of that material is paraphrased in this Geofile to provide context for the data presented.

New field observations and isotopic age determinations arising from the GEM project necessitate revisions to the stratigraphy that are still forthcoming and will be reported in future publications. In the interim, data included here provide a new timeline for the geological history of the Turtle Lake area:

- A new detrital zircon age from Horsefeed Formation tuffaceous limestone breccia of the Cache Creek terrane echoes a ~25 m.y. Carboniferous to Permian biochronological age

range, suggesting continuous additions to the volcanic substrate of the carbonate platform.

- Regional folds and thrusts affect Cache Creek terrane and Early to Middle Jurassic Laberge Group strata on the eastern flank of Stikinia. They are cut by the informally-named Lost Sheep peak intrusion, formerly considered Cretaceous, but now constrained by cooling ages on crosscutting lamprophyre dikes to Middle Jurassic. Lost Sheep peak intrusion is part of the regional Three Sisters plutonic suite.
- Strong fabric development in early phases of the Lost Sheep peak intrusion indicate that it was late syn- to post-kinematic, consistent with regional evidence for the age of the fold and thrust belt. Calc-alkalic lamprophyre dikes cut the Lost Sheep peak intrusion and surrounding Horsefeed Formation and have cooling ages of 168.2 ± 1.0 to 174.0±2.7 Ma.
- Cooling of the Lost Sheep peak intrusion through the argon diffusion in hornblende and biotite closure temperature occurred between ~166 – 162 Ma; a cooling rate of ~70° to 30°C/m.y. is implied.
- Only one dated igneous rock from the Turtle Lake area falls within the Late Jurassic to Early Cretaceous North American magmatic lull. It was collected from a granitic dike and returned an age of 145.75 ± 0.11 Ma.
- Cretaceous magmatism may have resumed by ~125 Ma in the Boundary Ranges to the west, but earliest records in the Turtle Lake area are a unimodal population of ~110 Ma detrital zircons from a karst deposit in Horsefeed limestone. None of the older zircons analyzed fall within the magmatic lull.
- A belt of Late Cretaceous volcanic rocks correlated with the Windy-Table suite is now dated at three sites as ~86.5 Ma, 80.63 ± 0.07 Ma and 79.7 ± 1.3 Ma.
- The crustal-scale, high-angle, Silver Salmon fault juxtaposes Cache Creek and Stikine terrane rocks and it affects rocks at the base of the Windy Table suite, constraining youngest motion to younger than ~86.5 Ma.
- The Silver Salmon fault is cut by the youngest recognized magmatic unit in the map area, a suite of quartz diorite stocks dated as 56.01 ±0.04 Ma and 56.12 ±0.29 Ma, coeval with magmatic rocks at the Engineer gold mine.

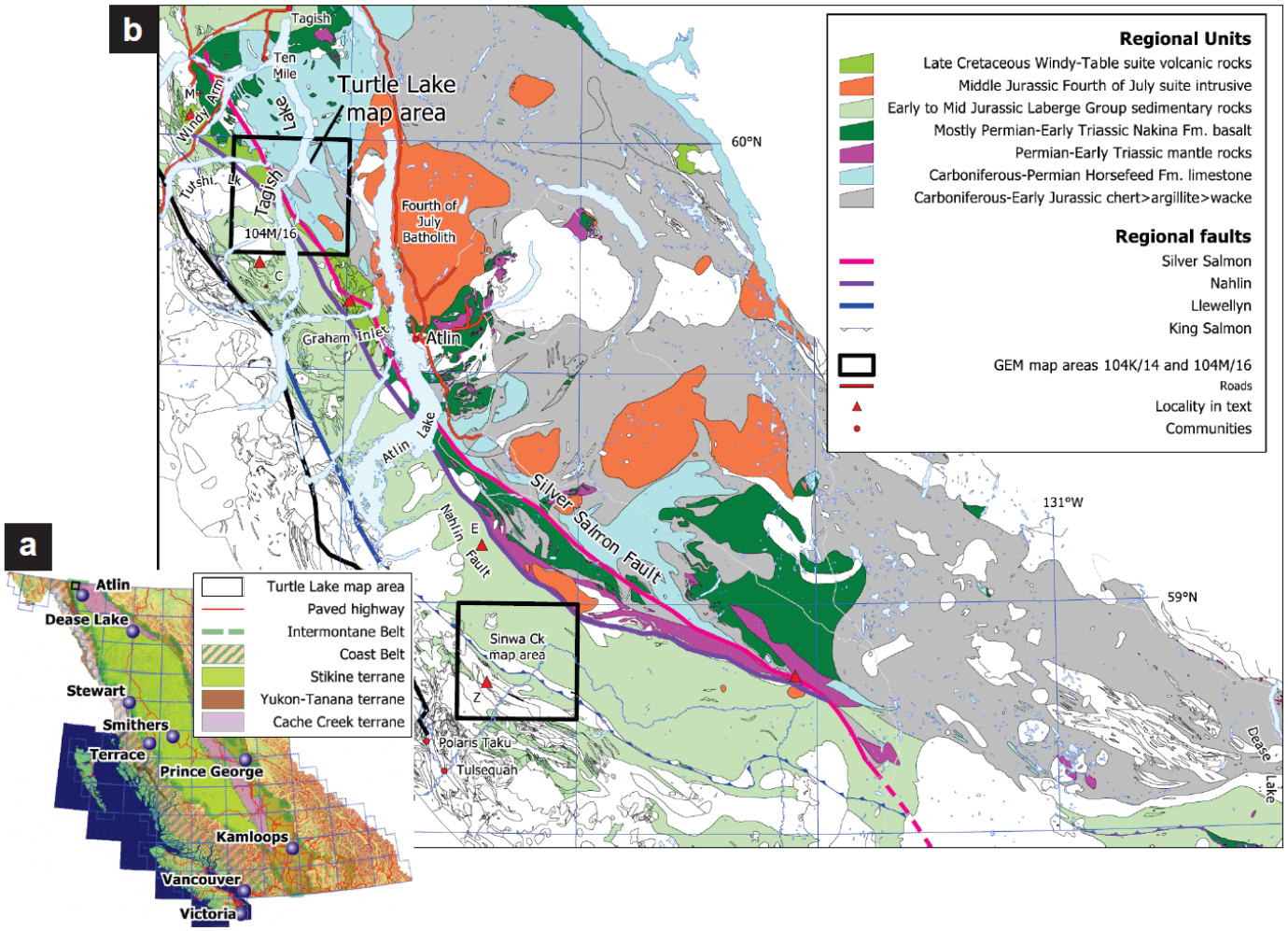

Fig. 1. a) Tectonic setting and location of the Turtle Lake map area in northwestern British Columbia. b) Regional geological setting showing the location of the quadrangles mapped as part of the Geo-mapping for Energy and Minerals initiative. Localities mentioned in the text are shown as labelled triangles: C – Mount Clive, E – Eclogite Ridge, M – Montana Mountain, Z – site of ~242 Ma detrital zircons in Mihalynuk et al. (2017). Figures unmodified from Mihalynuk et al. (2018).

Geochronological methods

U-Pb zircon chemical abrasion thermal ionization mass spectrometry (CA-TIMS)

CA-TIMS procedures are modified from Mundil et al. (2004), Mattinson (2005) and Scoates and Friedman (2008). Rock samples underwent standard mineral separation procedures, and zircon separates were handpicked in alcohol. The clearest, crack- and inclusion-free grains were selected, photographed, and then annealed at 900˚C for 60 hours. Annealed grains were chemically abraded, spiked with a $^{233\text{-}235}$U-^{205}Pb tracer solution (EARTHTIME ET535), and then dissolved. Resulting solutions were dried and loaded onto Re filaments (Gerstenberger and Haase, 1997).

Isotopic ratios were measured by a modified single collector VG-54R or 354S thermal ionization mass spectrometer equipped with analogue Daly photomultipliers. Analytical blanks were 0.2 pg for U and up to 1.0 pg for Pb. U fractionation was determined directly on individual

runs using the ET535 mixed $^{233\text{-}235}$U-^{205}Pb isotopic tracer. Pb isotopic ratios were corrected for fractionation of 0.30%/amu, based on replicate analyses of NBS-982 reference material and the values recommended by Thirlwall (2000). Data reduction used the Excel™-based program of Schmitz and Schoene (2007). Standard concordia diagrams were constructed and regression intercepts and weighted averages calculated with Isoplot (Ludwig, 2003). All errors are quoted at the 2σ or 95% confidence level, unless otherwise noted. Isotopic ages were calculated with the decay constants λ^{238}=1.55125E^{-10} and λ^{235}=9.8485E^{-10} (Jaffey et al, 1971). EARTHTIME U-Pb synthetic solutions were analysed on an ongoing basis to monitor accuracy.

U-Pb zircon Sensitive High Resolution Ion MicroProbe (SHRIMP) methods

Zircon separates were obtained using standard crushing, disk mill, Wilfley table, heavy liquid, and magnetic separation techniques. Analytical procedures and calibration details for the Sensitive High Resolution Ion Microprobe (SHRIMP) at the Geological Survey of Canada in Ottawa followed those described by Stern (1997) and Stern and Amelin (2003). Briefly, zircons were cast in a 2.5 cm diameter epoxy mount along with the Temora 2 zircon primary standard, the accepted ^{206}Pb/^{238}U age of which is 416.8 ± 0.33 Ma (Black et al., 2004). Fragments of the GSC laboratory zircon standard (z6266, with ^{206}Pb/^{238}U age = 559 Ma) were also included on the mount as a secondary standard, analyses of which were interspersed among the sample analyses throughout the data session to verify the accuracy of the U-Pb calibration. The mid-sections of the zircons were exposed using 9, 6, and 1 µm diamond compound, and the internal features of the zircons (such as zoning, structures, and alteration) were characterized in both back-scattered electron mode (BSE) and cathodoluminescence mode (CL) using a Zeiss Evo 50 scanning electron microscope. The mount surface was evaporatively coated with 10 nm of high purity Au. Analyses were conducted using an 16O- primary beam, projected onto the zircons at 10 kV. Before analysis, the ion beam was rastered over the area of interest for 2 minutes in order to locally remove the Au coating and eliminate effects of surface common lead. The sputtered area used for analysis was ~16 µm in diameter with a beam current of ca. 3.5 nA. The count rates at ten masses including background were sequentially measured over 6 scans with a single electron multiplier and a pulse counting system with deadtime of 23 ns. The 1σ external errors of ^{206}Pb/^{238}U ratios reported in the data table incorporate a ± 1.39% error in calibrating the standard Temora 2 zircon. Additional details of the analytical conditions and instrument settings are presented in the footnotes of the SHRIMP analysis tables included in this Geofile. Off-line data processing was accomplished using customized in-house software. Isoplot v. 3.00 (Ludwig, 2003) was used to generate concordia plots and to calculate weighted means. Errors for isotopic ratios in the Geofile tables are given at 1σ uncertainty, as are the apparent SHRIMP ages. Age errors reported in the text are at the 2σ uncertainty level and encompass the combined statistical uncertainty of the weighted mean age for the population and the 2σ error of the mean of the Temora 2 zircon calibration standard. No fractionation correction was applied to the Pb-isotope data; common Pb correction used the Pb composition of the surface blank (Stern, 1997). All ages are reported as the ^{207}Pb-corrected weighted mean ^{206}Pb/^{238}U age. The error ellipses on the concordia diagrams and the weighted mean errors are reported at 2σ.

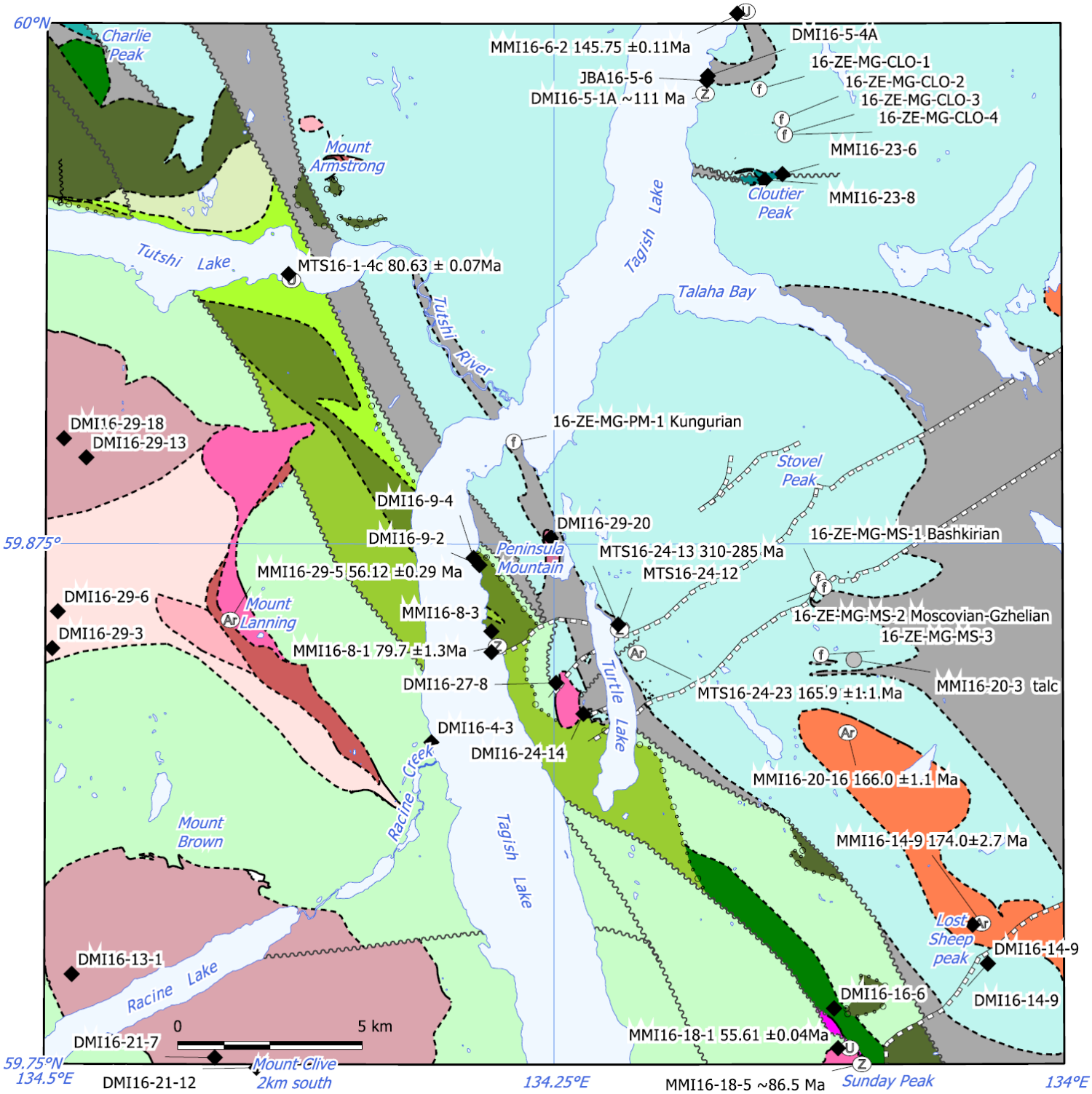

Fig. 2. Simplified geological map of the Turtle Lake map area (unmodified from Mihalynuk et al. 2018) with location of samples for which geochronology results are reported herein (sites denoted by U, Z and Ar). The legend for this figure is on the following page.

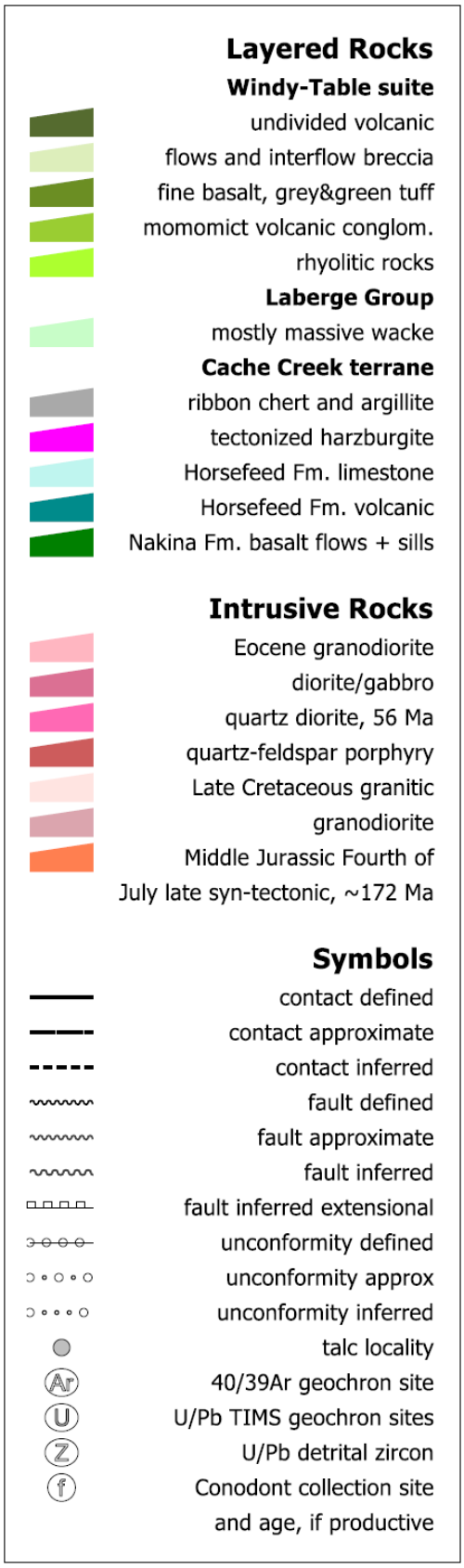

U-Pb zircon LA – ICPMS methods

Sample material selected was preferentially medium to coarse-grained sandstones which are expected to have the best likelihood of containing detrital zircons. Following collection, samples were isolated, double wrapped in plastic bags and placed in buckets. Samples were cleaned by washing followed by air abrading. Zircons were analyzed using laser ablation (LA) ICPMS methods using the techniques described by Tafti et al. (2009). Instrumentation comprised a New Wave UP-213 laser ablation system and a ThermoFinnigan Element2 single collector, double-focusing, magnetic sector ICPMS. All zircons greater than about 50 microns in diameter were picked from the mineral separates and mounted in an epoxy puck along with several grains of the Plešovice (337.13 ± 0.13 Ma, Sláma et al., 2007), and Temora2 (416.78 ± 0.33 Ma) zircon standards and brought to a very high polish. Before analysis, the surface of the mount was washed for 10 minutes with dilute nitric acid and rinsed in ultraclean water. The highest quality portions of each grain selected for analysis were free of alteration, inclusions, or possible inherited cores. Line scans rather than spot analyses were employed in order to minimize elemental fractionation during the analyses. A laser power level of 40% and a 25 μm spot size was used. Backgrounds were measured with the laser shutter closed for ten seconds, followed by data collection with the laser firing for approximately 35 seconds. The time-integrated signals were analysed using Iolite software (Patton et al, 2011), which automatically subtracts background measurements, propagates all analytical errors, and calculates isotopic ratios and ages. Corrections for mass and elemental fractionation are made by bracketing analyses of unknown grains with replicate analyses of the Plešovice zircon standard. A typical analytical session consisted of four analyses of the Plešovice standard zircon, followed by two analyses of the Temora2 zircon standard, five analyses of unknown zircons, two standard analyses, then five unknown analyses. Each session was completed with two Temora2 zircon standards and four Plešovice standard analyses. The Temora2 zircon standard was analysed as an unknown to monitor the reproducibility of the age determinations on a run-to-run basis (see Friedman et

Figure 2. Continued

al., 2016).

For analysis and plotting of detrital zircon results the ISOPLOT software of Ludwig (2003) is commonly used. Acceptance of the youngest PDP peak generated by Isoplot 4.15 as the DZMDA is typically a conservative approach, but not always (e.g. young single grain outlier in GMC14-60-2 identified by Isoplot as a sub-population). A more common issue may be the inclusion of multiple populations within a single PDP peak. Bandwidth is an important consideration in resolving PDPs, and proper bandwidth selection is important in identification of sub-populations. Routines such as Unmix in Isoplot 4.15 can be applied to help identify sub-populations, but this routine was not used here. To evaluate probability density distribution plots, we examined each sample dataset and considered criteria like smallest error envelopes and % discordance of individual zircon analyses in an attempt to reveal the youngest real zircon population(s). We applied a filter to some samples such that the youngest sub-population grains selected have 2σ errors less than 5% of the zircon age determination, and with $^{207}Pb/^{235}U$ and $^{206}Pb/^{238}U$ age determinations that differ by less than 1σ. We also considered zircon spot chemistry, placing more confidence in young sub-populations with homogeneous Pb, Th and U isotope contents as a percentage of the analytical counts per second compared to the range of values for that sample.

$^{40}Ar/^{39}Ar$ methods

Samples containing the freshest hornblende and biotite were broken in to pea-sized pieces using a hydraulic splitter and the pieces were pulverized in a hardened steel piston and sleeve apparatus. Single crystals were handpicked before irradiation. Standards and unknowns were placed in 2 mm deep wells in 18 mm diameter aluminium disks for irradiation in the cadmium-lined, in-core CLICIT facility of the Oregon State University TRIGA reactor. Standards were placed strategically so that the lateral neutron flux gradients across the disk could be evaluated. Irradiation duration was 10 hours. Standards used were Fish Canyon sanidine (28.2 Ma; Kuiper et al., 2008) and GA1550 biotite (98.5 Ma; Spell and McDougall, 2003). Planar regressions were fit to the standard data, and the $^{40}Ar/^{39}Ar$ neutron fluence parameter, J, interpolated for the unknowns. Uncertainties in J are estimated at 0.1 - 0.2% (1σ), based on Monte Carlo error analysis of the planar regressions (Best et al.,1995).

All $^{40}Ar/^{39}Ar$ analytical work was performed using a Thermo Fisher Scientific ARGUSVI multi-collector mass spectrometer, linked to a stainless steel Thermo Fisher Scientific extraction/purification line and Photon Machines (55 W) Fusions 10.6 CO_2 laser. Argon isotopes (from mass 40 to 37) were measured using Faraday detectors with low noise 1 x 10^{12} Ω resistors and mass 36 was measured using a compact discrete dynode (CDD) detector. Irradiated samples were placed in a Cu sample tray, with a KBr cover slip, in the extraction line under high vacuum and baked with an infrared lamp for 24 hours. Biotite analyses were performed on single crystals whereas hornblende analyses were performed on aliquots consisting of 3 crystals that were either fused or step-heated using the laser, and reactive gases were removed, after ~ 3 minutes, by three NP-10 SAES getters (two at room temperature and one at 450 °C) before being admitted to an ARGUSVI mass spectrometer by expansion. Five argon isotopes were measured simultaneously during a period of 6 minutes. Measured isotope abundances were corrected for extraction-line blanks, which were determined before every sample analysis. Line blanks averaged ~3.05 fA for mass 40 and ~0.01 fA for mass 36. The sensitivity for argon measurements is ~6.312 x 10^{17} moles/fA as determined from measured aliquots of Fish Canyon Sanidine (Dazé et al., 2003; Kuiper et al., 2008).

Mass discrimination was monitored by online analysis of air pipettes and gave a mean of D = 1.0035 ± 0.0014 per amu, based on 39 aliquots interspersed with the unknowns. A value of 295.5 was used for the atmospheric $^{40}Ar/^{36}Ar$ ratio (Steiger and Jaëger, 1977) for the purposes of routine measurement of mass spectrometer discrimination using air aliquots, and correction for atmospheric argon in the $^{40}Ar/^{39}Ar$ age calculation. Corrections were made for neutron-induced ^{40}Ar from potassium, ^{39}Ar and ^{36}Ar from calcium, and ^{36}Ar from chlorine (Roddick, 1983; Renne et al., 1998; Renne and Norman, 2001). Data collection was performed using Pychron (Ross, 2017) and data reduction, error propagation, age calculation and plotting were performed using MassSpec software (version 8.091; Deino, 2013). The decay constants used were those recommended by Steiger and Jäger (1977).

Geochronological results:

U-Pb Chemical Abrasion - Thermal Ionization Mass Spectroscopy

Sample # MMI16-6-2
Granitic dike, Tagish Lake, 145.75 ± 0.11 Ma
UTM coordinates: 546011m E, 6649818m N (NAD 83, UTM zone 8).

On the east shore of Tagish Lake, at a latitude of 60.003°N, a northwest-trending, orange-weathering, felsic, altered, medium- to coarse-grained feldspar porphyritic, ~40 cm thick dike cuts a strongly folded, cleaved and faulted section of chert and graphitic argillaceous strata (see Fig. 14a of Mihalynuk et al., 2018) to form rounded phacoids within a strongly sheared argillaceous matrix. Only brittle fractures with millimetres of offset affect the dike, which was collected to constrain the minimum age of deformation, as well as the crystallization age of the unusual dike lithology.
Analyses from four grains overlap concordia at 145.75 ± 0.11 Ma, and this precise date is considered the crystallization age of the dike.

Sample # MTS16-1-4c
Windy Table suite, rhyolite tuff, Tutshi Lake; 80.63 ± 0.07 Ma
UTM coordinates: 534680m E 6644710m N (NAD 83, UTM zone 8).

A white and rust-weathering rhyolite lapilli tuff (see Fig. 8a in Mihalynuk et al., 2018) on the south shore of eastern Tutshi Lake is interpreted as the lowest volcanic unit of the Windy Table suite exposed in that part of the map area (Fig. 2). We collected about 40 kg of fresh material from which zircons were separated. Five zircons were analyzed. Analytical results from the grains fall into two populations, with concordant U-Pb isotopic ratios and mutually overlapping error 2σ ellipses. Two grains are between 80.8 and 81 Ma, and three grains are at 80.63 ± 0.07 Ma, which we interpret as the crystallization age of the unit. The older population likely represents precursor magmatic products cannibalized during migration and eruption of the rhyolite magma.

Sample # MMI16-18-1
Sunday Peak stock quartz diorite; 80.63 ± 0.07 Ma
UTM coordinates: 550280m E 6624344m N (NAD 83, UTM zone 8).

The Sunday Peak stock is one of a suite of zoned granodioritic to dioritic intrusions (see Fig. 10a in Mihalynuk et al., 2018) that cut the Whitehorse trough. On the basis of lithologic similarity and sparse K-Ar geochronology (e.g., Bultman, 1979, recalculated in Breitsprecher and Mortensen, 2004), these intrusions have formerly been considered mainly Late Cretaceous (Mihalynuk et al., 1996, 1999). At Sunday Peak, a ~0.6 km^2 stock cuts and thermally metamorphoses rocks on both sides of a terrane-bounding fault: harzburgite of the Cache Creek terrane and wacke of Whitehorse trough (that has historically been considered as overlapping the Stikine terrane) plus overlapping Windy-Table suite felsic volcanic conglomerate. Thus, an age

determination from the stock constrains the latest phase of major fault motion as well as the age of overlapping the conglomerate. Four zircons were analyzed. All have concordant U-Pb isotopic ratios with mutually overlapping error 2σ ellipses, producing a precise age of 55.61 ± 0.04 Ma.

Detrital zircon SHRIMP

Sample # DMI16-5-1A
Horsefeed Formation hematitic breccia matrix; ~111 Ma
UTM coordinates: 546012m E 6649818m N (NAD 83, UTM zone 8).

We collected samples of the laminated hematitic calcarenite matrix to breccias in the Horsefeed Formation from exposures along the eastern shoreline of Tagish Lake (Fig. 2, for sampled material see Fig. 4b in Mihalynuk et al., 2018) and from a low ridge south of Stovel Peak (Fig. 2, for photo of rock see Fig. 4c in Mihalynuk et al., 2018). Petrographic work showed that the ridge sample contains only rare quartz grains, so the lakeshore sample, with more abundant quartz grains, was analyzed with the expectation that detrital zircon contents would be proportional to the abundance of quartz grains.
Of the zircon grains recovered from the lakeshore sample, 124 grains were selected and mounted for analysis. A majority of these grains are clear and pale brown in colour, and are euhedral well-faceted equant, stubby, and elongate prisms. About 10% of the grains have rounded grain boundaries. Clear bubble- and rod-shaped inclusions, and brown bubble-shaped inclusions are relatively common. In SEM-cathodoluminescence (CL) images, most grains exhibit distinct oscillatory zoning, and lesser sector zoning. CL response from the grains varies from very dark (relatively high U content) to bright (relatively low U content). Cores are visible in ~10% of the grains. Of the zircon grains analyzed, the youngest population is 111 Ma, and the youngest grain 107 Ma. This age is nearly 150 m.y. younger than the youngest known age limit of the Horsefeed Formation., based on Late Permian fossils south of the mouth of Talaha Bay (Monger, 1975). We interpret the hematitic breccia as Cretaceous karst infill representing a period exposure.

Sample # MMI16-16-9
Windy Table suite, felsic volcanic conglomerate and breccia at Sunday Peak; ~85 Ma
UTM coordinates: 550621m E 6623917m N (NAD 83, UTM zone 8).

Conglomeratic, reworked felsic volcanic breccia (see Mihalynuk et al., 2018, Fig. 18a) occurs east of Sunday Peak between Laberge Group sedimentary rocks to the west and harzburgite mantle tectonite to the east (Fig. 2). An unconformable contact with the harzburgite was established on the basis of serpentinite clasts in the conglomerate and dikelets of volcanic breccia in the harzburgite (see Mihalynuk et al., 2018, Fig. 7a inset). However, contact relations between the volcanic conglomerate and breccia and the adjacent rocks of the Laberge Group are masked by deformation and subsequent thermal alteration by the Sunday Peak stock (see Mihalynuk et al., 2018, Fig. 7d). Consequently, it was unclear if the volcanic conglomerate was an intraclast-bearing layer within the Laberge Group that had lapped against harzburgite exposed in the Early to Middle Jurassic. If part of the Laberge Group, then stratigraphic and structural continuity since Middle Jurassic could be established (with strong post-deformational shearing along the Laberge

wacke and Harzburgite – conglomerate contacts resulting in a relative offset that is less than the footprint of the felsic conglomerate unit). A sample ~ 25 cm in diameter of the stratigraphically lowest conglomerate containing almost entirely felsic volcanic clasts was collected for detrital zircon analysis.

Approximately 120 grains were mounted for analysis, representing a full range of zircon morphologies (see Mihalynuk et al., 2018, Fig. 18b). A majority of grains are clear and colourless, equant to stubby prisms with well-preserved facets and minor clear bubble-shaped inclusions. In SEM-CL images, most grains exhibit distinct oscillatory zoning. Sector zoning is present in one third of the crystals. Core-like regions are seen in ~10% of the grains. A maximum depositional age is given by three Late Cretaceous grains. The youngest of the three grains is 84 Ma, whereas their combined weighted average age is 85 Ma. Grain 81 has a high-U, 86.5 Ma rim, and a 216 Ma core with lower U content (see Mihalynuk et al., 2018, Fig. 18b). We interpret the youngest zircons to represent the age of syn-volcanic deposition and correlate the unit with strata of the same age (85.0 ±1.8 Ma) near the base of the Windy-Table suite, as recently shown by Zagorevski et al. (2017).

U-Pb Laser Ablation-Inductively-Coupled Plasma Mass Spectroscopy

Sample # MTS16-24-13
Horsefeed Formation, tuffaceous limestone breccia east of Turtle Lake; <~285 Ma
UTM coordinates: 543823m E 6635458m N (NAD 83, UTM zone 8).

Green and grey-weathering tuffaceous limestone breccia underlies the slopes east of northern Turtle Lake. Outcrop compositions range from predominantly volcanic to limestone clast-bearing. A sample was collected from a volcanic-rich protolith that contained both aphanitic green and cream-coloured, lapilli-sized volcanic clasts as well as angular limestone and rare chert (see Fig. 19a in Mihalynuk et al., 2018). Of the zircon grains separated, 39 were suitable for LA-ICPMS analysis (Table 5); all were angular fragments with strong growth-zoning (see Mihalynuk et al., 2018, Figs. 19b, c). The zircon fragments returned an age distribution with a peak at ~295 Ma (37 grains), and a minor ill-defined sub population at ~310 Ma (2 grains). Nearly two of three grains (64%) display overlapping $^{206}Pb/^{238}U$ (2σ <5%) and $^{207}Pb/^{235}U$ (2σ <10%) ages, and $^{207}Pb/^{206}Pb$ ages that are geologically meaningful and concordant within error. Five of these grains cluster at ~285 Ma, which we interpret as the best estimate of the maximum depositional age.

Sample # MMI16-8-1
Windy-Table suite volcanic rocks at Peninsula Mountain; 79.7 ±1.3 Ma
UTM coordinates: 540468m E 6634980m N (NAD 83, UTM zone 8).

Volcaniclastic strata crop out on the west side of Peninsula Mountain and are well exposed along the shore of Tutshi Lake. Contacts with Laberge Group wacke and argillite to the south are not exposed, but to the north, a fault zone containing panels of chert and argillite juxtapose the unit with limestone of the Horsefeed Formation. Age relations are ambiguous, but most previous workers considered the Peninsula Mountain volcanic strata to be Triassic. Reasons to doubt the Triassic age assignment arose during the field program: tuffaceous and conglomeratic sections at Peninsula Mountain are lithologically similar to strata of probable Cretaceous age to the north and south in the Turtle Lake map area, and strata of presumed Triassic age a few km outside the southeast corner of the map area, were found to be Cretaceous and correlated with the Windy-Table suite (Zagorevski et al., 2017). To address the uncertainty about the affiliation of volcanic rocks at Peninsula Mountain, we collected a sample of grey-green feldspar-pyroxene-phyric breccia (see Mihalynuk et al., 2018, Fig. 9b) for LA-ICPMS analysis.

Six usable zircons were recovered and analyzed; collectively they define an age of 79.7 ± 1.3 Ma, consistent with Late Cretaceous, not Triassic deposition.

$^{40}Ar/^{39}Ar$ step heating

Sample # MMI16-20-16
Synkinematic Lost Sheep peak intrusion; 166.0 ±1.1 Ma (hornblende cooling)
UTM coordinates: 550127m E 6632781m N (NAD 83, UTM zone 8).

The Lost Sheep peak intrusion is a variably foliated, 2.5 km by >9 km, northwest elongated body in the southeast corner of the Turtle Lake map area. It probably averages granodiorite composition, but ranges from gabbro to granitic with mafic phases tending to be the most intensely foliated. Pegmatitic granitic phases are not foliated but comingle with the variably sheared mafic to intermediate enclaves (see Mihalynuk et al., 2018, Fig. 10c). Fine- to medium-grained hornblende and biotite can comprise more than 30% of the rock and tend to be intimately intergrown, together with titanite (<1% ~4%). We sampled the freshest part of an intermediate, foliated phase of the intrusion, ~400 m from the northeastern contact with the aim of obtaining a post-deformational cooling age.

Separates of both biotite and hornblende were hand-picked. Selected biotite grains yielded a plateau age of 161.61 ±0.85 Ma, which considers 100% of ^{39}Ar released. Hornblende separated from this sample returned an age of 166.0 ±1.1 Ma from 81.7 % of ^{39}Ar liberated.

Sample # MMI16-29-05
Biotite quartz diorite at Mount Lanning; 56.12 ±0.29 Ma (biotite cooling)
UTM coordinates: 533100m E 6635600m N (NAD 83, UTM zone 8).

Fresh, unfoliated, medium- to fine-grained, leucocratic, biotite quartz diorite (see Mihalynuk et al., 2018, Fig. 22a) appears to be one of the latest phases of the ~160 km^2 intrusion that underlies Mount Lanning. It cuts and thermally metamorphoses deformed Laberge Group strata. It is a northwest-trending pluton with an irregular outline, except in the south where it is a southward-tapering, steeply dipping tabular body that terminates near Racine Creek (Fig. 2). It is one of the largest intrusive domains lacking published isotopic age work. A clean separate of vitreous, elastic, black biotite was obtained.

Analysis of two biotite grains yielded statistically identical results of: 56.12 ±0.29 Ma from 100% of the ^{39}Ar released and 55.99 ±0.29 Ma from 97.7% of ^{39}Ar released. The fresh mineralogy and field relationships of the quartz diorite at Mount Lanning are consistent with the young, Eocene age.

Sample # MMI16-14-9
Lamprophyre dike at Lost Sheep peak; 174.0±2.7 Ma (hornblende cooling)
UTM coordinates: 553871m E 6627723m N (NAD 83, UTM zone 8).

Lamprophyre dikes have a long-established association with gold mineralization (e.g. Young, 1948; Rock and Groves, 1988), although their role in gold deposit genesis is not without controversy (e.g., Kerrich and Wyman, 1994). In the Atlin gold camp, altered lamprophyre dikes

are found with lode gold mineralization at the Yellowjacket deposit, and are intimately associated with precious metal-rich base metal sulphide veins at the Atlin Ruffner mine (past producing), where they cut weakly deformed granodiorite of the Fourth of July batholith. Considering such precious metal affiliation, we selected two sites for geochronological investigation: conspicuous southwest-trending lamprophyre dikes that cut the intrusion at Lost Sheep peak (MMI16-14-9), and limestone near Turtle Lake (see following sample).

On steep faces of Lost Sheep peak lamprophyre dikes are well exposed in fresh landslide scars, but otherwise tend to be weathered slots floored with biotite-rich gruss in the host granodiorite. We sampled the thickest (~15m) and freshest of the well-exposed biotite-rich dikes (possibly a composite of superimposed dikes) on the northeast flank of Lost Sheep peak. The dike is dark green to black, medium- to coarse-grained and has a knobbly weathered appearance due to an abundance of xenoliths, xenocrysts, xenocryst aggregates (see Mihalynuk et al., 2018, Fig. 23a), and calcite filled amygdales or ocelli. We picked the freshest and highest purity hornblende and biotite grains to obtain clean separates for $^{40}Ar/^{39}Ar$ age determination, but microscopic intergrowths of the two minerals and pyroxene (see Mihalynuk et al., 2018, Figs. 23b, c) likely escaped detection.

Step heating of the best quality biotite grain produced an age of 168.2 ± 1.0 Ma from 75.8% of ^{39}Ar released. Hornblende analyses returned an age of 174.0±2.7 Ma from 74.5% of ^{39}Ar released, the preferred interpreted age for this sample. Results from a second hornblende aliquot were rejected, but integrating all ^{39}Ar from both hornblende aliquots yields an age of 171 ±10 Ma.

Sample # MTS16-24-23
Lamprophyre dike at Turtle Lake, 165.9 ±1.1 Ma (biotite cooling)
UTM coordinates: 542755m E 6633812m N (NAD 83, UTM zone 8).

Extensively diked limestone on the steep slope above eastern Turtle Lake includes fine to medium-grained lamprophyre. Intimate mineral intergrowths precluded isolation of pure mineral separates, but about 10 grains of visually pure biotite were obtained. Even then, the coarsest biotite grains are rutilated (see Mihalynuk et al., 2018, Fig. 23e). A separate of intergrown hornblende and biotite was also obtained for total fusion analysis, but was not used. The best quality biotite grain yielded a release spectrum from which consideration of 100% of the gas gives an $^{40}Ar/^{39}Ar$ age of 163.6 ±2.2 Ma. Removal of the first three steps yields an age of 162.80 ±0.93 Ma from 53.9% of ^{39}Ar released. Rejection of the first step yields and age of 165.9 ±1.1 Ma, and is probably closest to the actual crystallization age of the dike.

References

Best, M.G., Christiansen, E.H., Deino, A.L., Grommé, C.S., Tingey, D.G., 1995. Correlation and emplacement of a large, zoned, discontinuously exposed ash fl ow sheet; the $^{40}Ar/^{39}Ar$ chronology, paleomagnetism, and petrology of the Pahranagat Formation, Nevada. Journal of Geophysical Research, 100, 24593-24609.

Black, L.P., Kamo, S.L., Allen, C.M., Davis, D.W., Aleinikoff, J.N., Valley, J.W., Mundil, R., Campbell, I.H., Korsch, R.J., Williams, I.S. and Foudoulis, C., 2004. Improved $^{206}Pb/^{238}U$ microprobe geochronology by the monitoring of a trace-element-related matrix effect; SHRIMP, ID–TIMS, ELA–ICP–MS and oxygen isotope documentation for a series of zircon standards. Chemical Geology, 205, 115-140.

Breitsprecher, K., and Mortensen, J.K., 2004. BCAge 2004A-1-a database of isotopic age determinations for rock units from British Columbia. British Columbia Ministry of Energy and Mines, British Columbia Geological Survey, Open File, v. 3.

Bultman, R.B., 1979. Geology and tectonic history of the Whitehorse Trough west of Atlin, British Columbia. Unpublished Ph.D. thesis, Yale University, 284 p.

Dazé, A., Lee, J.K., and Villeneuve, M., 2003. An intercalibration study of the Fish Canyon sanidine and biotite $^{40}Ar/^{39}Ar$ standards and some comments on the age of the Fish Canyon Tuff. Chemical Geology, 199, 111-127.

Deino, A.L. 2013. Users manual for Mass Spec v. 7.961: Berkeley Geochronology Center Special Publication 1a, 132 p.

Crowley, J.L., Schoene, B. and Bowring, S.A. 2007. U-Pb dating of zircon in the Bishop Tuff at the millennial scale. Geology, 35, 1123-1126.

Friedman, R.M., Mihalynuk, M.G., Diakow, L.J., and Gabites, J.E., 2016. Southern Nicola Arc Project 2015: Geochronologic data constraining Nicola arc history along a transect near 50°N. British Columbia Ministry of Energy and Mines, British Columbia Geological Survey GeoFile 2016-3.

Gerstenberger, H. and Haase, G. 1997. A highly effective emitter substance for mass spectrometric Pb isotopic ratio determinations. Chemical Geology, 136, 309-312.

Jaffey, A.H., Flynn, K.F., Glendenin, L.E., Bentley, W.C. and Essling, A.M., 1971. Precision measurement of half-lives and specific activities of ^{235}U and ^{238}U. Physics Review, C4, 1889-1906.

Kerrich, R., and Wyman, D.A., 1994. The mesothermal gold-lamprophyre association: significance for an accretionary geodynamic setting, supercontinent cycles, and metallogenic processes. Mineralogy and Petrology, 51, 147–172.

Kuiper, K.F., Deino, A., Hilgen, F.J., Krijgsman, W., Renne, P.R., and Wijbrans, J.R., 2008. Synchronizing rock clocks of Earth history. Science, 320, 500-504.

Logan, J.M., and Mihalynuk, M.G., 2014. Tectonic controls on Early Mesozoic paired alkaline porphyry deposit belts (Cu-Au ± Ag-Pt-Pd-Mo) within the Canadian Cordillera. Economic Geology, Special Issue on Alkalic Porphyry Deposits, v. 109, p. 827-858.

Ludwig, K.R., 2003. Isoplot 3.09: a geochronological toolkit for Microsoft Excel. Berkeley Geochronology Center, Special Publication 4, Berkeley.

Mattinson, J.M., 2005. Zircon U-Pb chemical abrasion (CA-TIMS) method: combined annealing and multi-step partial dissolution analysis for improved precision and accuracy of zircon ages. Chemical Geology, 220, 47-66.

Mihalynuk, M.G., Bellefontaine, K.A., Brown, D.A., Logan, J.M., Nelson, J.L., Legun, A.S., and Diakow, L.J., 1996. Geological compilation, northwest British Columbia (NTS 94E, L, M; 104F, G, H, I, J, K, L, M, N, O, P; 114J, O, P). British Columbia Ministry of Energy and Mines, British Columbia Geological Survey Open File 1996-11.

Mihalynuk, M.G., P. Erdmer, Ghent, E.D., Cordey, F., Archibald, D.A., Friedman, R.M., Johannson, G.G., 2004. Coherent French Range blueschist: Subduction to exhumation in < 2.5 m.y.? Geological Society of America Bulletin, 116, 910–922. doi:10.1130/b25393

Mihalynuk, M.G., Mountjoy, K.J., Smith, M.T., Currie, L.D., Gabites, J.E., Tipper, H.W., Orchard, M.J., Poulton, T.P., and Cordey, F., 1999. Geology and mineral resources of the Tagish Lake area (NTS 104M/ 8,9,10E, 15 and 104N/ 12W), northwestern British Columbia. British Columbia Ministry of Energy and Mines, British Columbia Geological Survey, Bulletin 105, 202 p.

Mihalynuk, M.G., Nelson, J. and, Diakow, L.J., 1994. Cache Creek Terrane entrapment: oroclinal paradox within the Canadian Cordillera. Tectonics, 13, 575–595.

Mihalynuk, M.G., Zagorevski, A., English, J.M., Orchard, M.J., Bidgood, A., K., Joyce, N., and Friedman, R.M., 2017. Geology of the Sinwa Creek area, northwest BC (104K/14). In: Geological Fieldwork 2016, British Columbia Ministry of Energy and Mines, British Columbia Geological Survey Paper 2017-1, pp. 153–178.

Mihalynuk, M.G., Zagorevski, A., Milidragovic, D., Tsekhmistrenko, M., Friedman, R.M., Joyce, N., Camacho, A., and Golding, M., 2018. Geologic and geochronologic update of the Turtle Lake area, NTS 104M/16, northwest British Columbia. In: Geological Fieldwork 2017, British Columbia Ministry of Energy, Mines and Petroleum Resources, British Columbia Geological Survey Paper 2018-1, pp. 83-128.

Monger, J., 1975. Upper Paleozoic rocks of the Atlin Terrane, northwestern British Columbia and south-central Yukon. Geological Survey of Canada, Paper 74-47, 63 p.

Mundil,R., Ludwig, L.R., Metcalfe, I. and Renne, P.R., 2004. Age and timing of the Permian mass extinctions: U/Pb dating of closed system zircons. Science, 305, 1760-1763.

Patton, C., Hellstrom, J., Paul, B., Woodhead, J. and Hergt, J., 2011. Iolite: freeware for the visualization and processing of mass spectrometry data. Journal of Analytical Atomic Spectroscopy, 26, 2508-2518.

Renne, P.R., and Norman, E.B., 2001. Determination of the half-life of ^{40}Ar by mass spectrometry. Physical Review C, 63, 047302.

Renne, P.R., Swisher, C.C., III, Deino, A.L., Karner, D.B., Owens, T. and DePaolo, D.J., 1998. Intercalibration of standards, absolute ages and uncertainties in ^{40}Ar/^{39}Ar dating. Chemical Geology, 145, No. 1-2, 117-152.

Rock, N.M., and Groves, D.I., 1988. Do lamprophyres carry gold as well as diamonds? Nature, 332, 253–255.

Roddick, J.C., 1983. High precision intercalibration of ^{40}Ar-^{39}Ar standards. Geochimica Cosmochimica Acta, 47, 887-898.

Ross, J., 2017. Pychron documentation. New Mexico Institute of Mining and Technology, 115 p. <https://media.readthedocs.org/ pdf/pychron/latest/pychron.pdf> Last accessed January 11, 2018.

Schmitz, M.D. and Schoene, B., 2007. Derivation of isotope ratios, errors, and error correlations for U-Pb geochronology using ^{205}Pb-^{235}U(^{233}U)-spiked isotope dilution thermal ionization

mass spectrometric data. Geochemistry, Geophysics, Geosystems, 8, Q08006.doi:10.1029/2006GC001492.

Scoates, J.S. and Friedman, R.M., 2008. Precise age of the plantiniferous Merensky Reef, Bushveld Complex, South Africa, by the U-Pb ID-TIMS chemical abrasion technique, Economic Geology, 103, 465-471

Slama, J., Kosler, J., Condon, D.J., Crowlley, J.L., Gerdes, A., Hanchar, J.M., Horstwood, M.S.A., Morris, G.A., Nasdala, L., Norberg, N., Schaltegger, U., Xchoene, B., Tubrett, M.N. and Whitehouse, M. J., 2007. Plesovice zircon – A new natural reference material for U-Pb and Hf isotopic microanalysis. Chemical Geology, 249, 1-35.

Spell, T.L., and McDougall, I., 2003. Characterization and calibration of $^{40}Ar/^{39}Ar$ dating standards. Chemical Geology, 198, 189-211.

Steiger R.H., and Jäger E., 1977. Subcommission on geochronology: convention on the use of decay constants in geo- and cosmochronology. Earth and Planetary Science Letters, 36, 359-362.

Stern, R., 1997. The GSC Sensitive High Resolution Ion Microprobe (SHRIMP): Analytical techniques of zircon U-Th-Pb age determinations and performance evaluation. In: Radiogenic Age and Isotopic Studies, Report 10, Geological Survey of Canada, Current Research 1997-F, pp. 1–31.

Stern, R.A., and Amelin, Y., 2003. Assessment of errors in SIMS zircon U–Pb geochronology using a natural zircon standard and NIST SRM 610 glass. Chemical Geology, 197, 111–142.

Tafti, R., Mortensen, J.K., Lang, J.R., Rebagliati, M. and Oliver, J.L., 2009. Jurassic U-Pb and Re-Os ages for newly discovered Xietongmen Cu-Au porphyry district, Tibet: implications for metallogenic epochs in the southern Gangdese Belt. Economic Geology, 104, 127-136.

Thirlwall, M.F. 2000. Inter-laboratory and other errors in Pb isotope analyses investigated using a 207Pb-204Pb double spike. Chemical Geology, 163, 299-322.

Young, J.W., 1948. The relationship between lamprophyre dykes and ore deposits with special reference to British Columbia. Unpublished M.A.Sc. thesis, The University of British Columbia, 184 p.